Optical Reflectance and Scattering Studies of Nucleation and Growth of Bubbles at a Liquid-Solid Interface Induced by Pulsed Laser Heating

Oguz Yavas and Paul Leiderer
Department of Physics, University of Konstanz, W-7750 Konstanz, Germany

Hee K. Park and Costas P. Grigoropoulos
Department of Mechanical Engineering, University of California, Berkeley, California 94720

Chie C. Poon, Wing P. Leung, Nhan Do, and Andrew C. Tam
IBM Almaden Research Center, 650 Harry Road, San Jose, California 95120-6099
(Received 30 November 1992)

Optical reflectance and light scattering measurements are used to study bubble nucleation of various liquids and subsequent explosive vaporization at the surface of a thin chromium film heated by a 248-nm KrF excimer laser. Liquids studied include water, ethanol, methanol, isopropanol, and different mixtures of water and isopropanol. The reflectance and scattering signals show distinct transients when the excimer laser fluence exceeds a certain liquid-dependent threshold. The reflectance signals are analyzed to provide bubble growth kinetics and explosive vaporization thresholds of the liquids.

PACS numbers: 62.60.+v, 68.35.Rh, 78.20.Hp, 82.40.Fp

The thermophysics of superheated pure or mixed liquids has been a subject of interest for many years. Different aspects such as the universal behavior, the kinetic and thermodynamic superheat limits, and the critical parameters have been studied extensively [1–3]. Here we present, for the first time to our knowledge, the application of optical reflectance and scattering techniques to the study of the nucleation dynamics and explosive vaporization of various liquids on an opaque solid surface that is heated by a short laser pulse. This process is also of technical interest, since, as recently reported, this kind of liquid explosion can efficiently be used to remove submicron sized particles from solid surfaces [4].

The experimental setup is shown in Fig. 1. The 248-nm KrF excimer laser pulse (FWHM $\sim$16 ns) is directed at normal incidence onto the sample and irradiates a relatively large area (1×1 cm^2). The probe beam is directed to the center of this area at an angle of incidence in the liquid, θ, adjustable from 7° to 46°. The specular reflectance and the scattered light can be detected simultaneously using fast photodetectors (rise time <1 ns) and monitored on a digital storage oscilloscope (Tektronix TDS540). Several liquids including water, isopropanol (IPA), ethanol, methanol, and different mixtures of water and IPA have been studied. The absorbing sample is a 0.2 μm thick chromium film on a sapphire substrate.

We observe no change on the probe beam reflectance when the sample is irradiated in air for excimer laser fluences up to 100 mJ/cm^2, indicating that the optical properties of the chromium film are not temperature dependent for the temperature range achieved. For the case of a liquid in contact with the chromium film, the reflectance signal remains unchanged by irradiation at low excimer laser fluences. When the fluence exceeds a certain liquid-dependent threshold F_{th}, however, a transient change of the reflectance signal is observed as shown

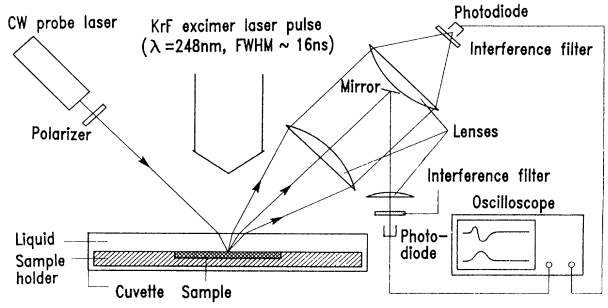

FIG. 1. Experimental arrangement for optical reflectance and scattering probing of formation and growth of bubbles induced by pulsed laser heating.

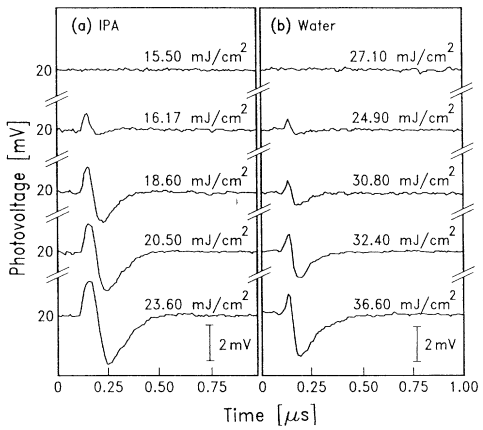

FIG. 2. Transient reflectance signal with increasing excimer laser fluence for 0.2 μm chromium film, $\lambda_{probe}=752$ nm, s polarized, $\theta=7°$: (a) IPA, (b) water.

in Fig. 2. Similar transients, with minor differences as discussed below, are obtained for all the investigated liquids. The shape of the transient signal depends on the angle of incidence and polarization of the probe beam. For small angles of incidence the same shape for the transient reflectance signal is observed for both s- and p-polarized probe beams: an abrupt reflectance increase followed by a more gradual dip. At incident angles larger than 40°, however, the leading positive part of the signal is only observable for the s-polarized probe beam. We have verified that the observed signals in Fig. 2 are not due to deflection of the reflected probe beam by performing tests using a knife edge in front of the photodiode. Furthermore, the scattering signal shows a peak which coincides with the timing of the reflectance dip. An example for simultaneously measured transient reflectance and scattering signal is shown in Fig. 3.

The transient reflectance signal can be explained as follows: Because of the fast heating process, superheating of the liquid above the usual boiling point is expected, until nucleation of the bubbles sets in at a "cloud point," which marks the limit of supersaturation, as is observed during phase separation in a supersaturated fluid [5]. As a result, a uniform layer of bubbles is created at the surface of the Cr film. Initially, the radius of the bubbles is much smaller than the probe beam wavelength, and the bubble growth is inertia controlled [1,6]. In this initial stage of bubble growth, as long as the bubble radius $R \ll \lambda_{\text{probe}}/2\pi n_{\text{liq}}$, Rayleigh scattering dominates [7,8], where n_{liq} is the refractive index of the liquid. Depending on the angle of incidence and polarization of the probe beam, an increase or decrease of the reflectance can be observed. At later time when bubbles grow in size, $R \gg \lambda_{\text{probe}}/2\pi n_{\text{liq}}$, Mie scattering becomes important [7,8]. This results in a decrease of the specular reflectance. After a certain period of time and having reached a certain radius, some of the bubbles detach from the chromium surface or collapse randomly so that scattering losses are reduced gradually and the reflectance signal returns to the initial level.

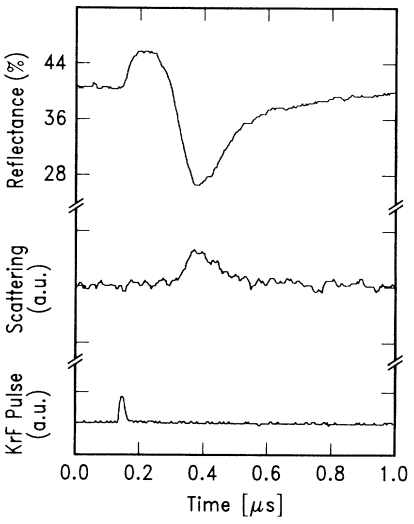

FIG. 3. Transient reflectance (top curve) and scattering (middle curve) signal for methanol. $\lambda_{\text{probe}} = 632.8$ nm, unpolarized, $\theta = 26°$. Lower curve represents the KrF excimer pulse ($F = 56.3$ mJ/cm^2).

The curves in Fig. 4 are calculated according to the effective medium theory by Maxwell Garnett [9], considering the ensemble of small bubbles and the liquid as a medium with an effective dielectric constant:

$$\varepsilon_{\text{eff}} = \varepsilon_l \left(1 - \frac{3f(\varepsilon_l - \varepsilon_v)}{2\varepsilon_l + \varepsilon_v + f(\varepsilon_l - \varepsilon_v)} \right),$$

where f is the fractional volume of bubbles, and ε_l and ε_v are the dielectric constants for liquid and vapor, respectively. Two basic assumptions are needed: The bubble radius has to be much smaller than the probe beam wavelength and macroscopically the bubbles must be distributed uniformly in the liquid. These conditions are met at the beginning of the bubble growth and the system can be considered as multilayered consisting of a bulk liquid (5 mm thick), a "foamy" liquid film (0.05–1 μm thick) with an effective dielectric constant ε_{eff}, a chromium film (0.2 μm thick), and a sapphire substrate (250 μm thick). Using thin film optics we have calculated the reflectance for such a system for different angles of incidence, polarizations, and different thickness and bubble content of the foamy film. The results confirm the experimentally observed increase or decrease of the reflectance with increasing fractional volume depending on the angle of incidence and polarization of the probe beam.

It has been shown that the bubble radius increases linearly with time during the initial inertia-controlled stage of growth, and increases with the square root of time in the later heat-transfer-controlled stage [1,6]. By assuming that the transition from Rayleigh to Mie scattering occurs when the bubble radius equals $\lambda_{\text{probe}}/2\pi n_{\text{liq}}$ ($\equiv R_{\text{tr}}$), and that the time for the first reflectance

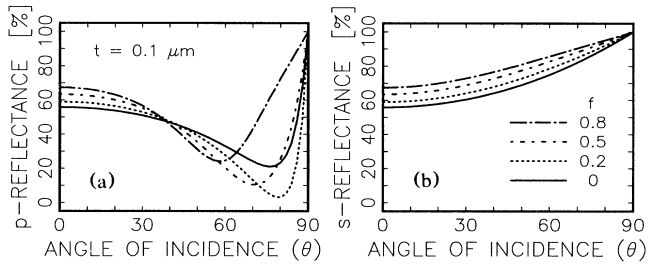

FIG. 4. The results of calculations based on the effective medium theory (Maxwell Garnett) for reflectance vs incident angle for a 0.1 μm thick foamy film on 0.2 μm thick chromium film on a sapphire substrate immersed in water. The optical properties of bulk Cr are used in the calculation [14]. t is the thickness of the foamy liquid film, f is the fractional volume of the bubbles, $\lambda_{\text{probe}} = 632.8$ nm: (a) p polarized, (b) s polarized.

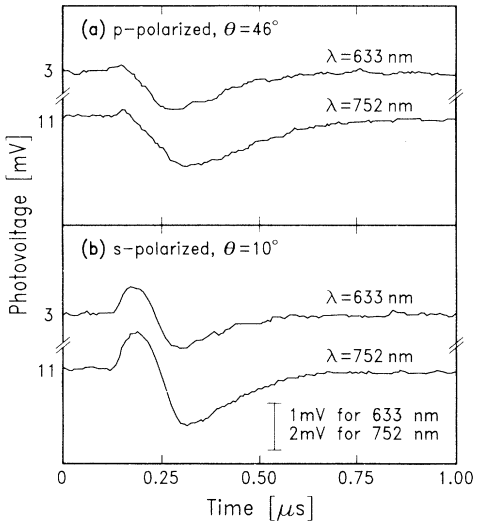

FIG. 5. Comparison of the reflectance transient for IPA at two different probe beam wavelengths. $F=22.4$ mJ/cm^2. (a) $\theta=46°$, p polarized; (b) $\theta=10°$, s polarized.

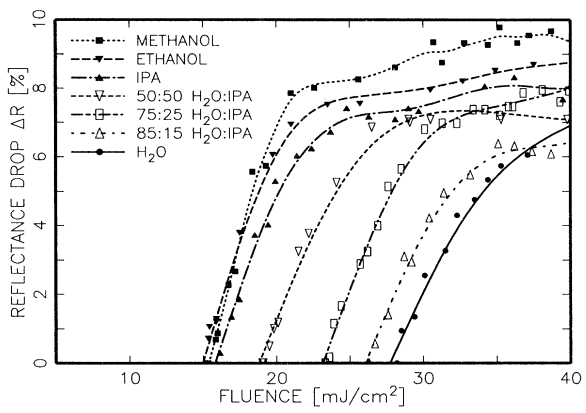

FIG. 6. Explosion threshold behavior for different liquids at the surface of a 0.2 μm thick chromium film on a sapphire substrate irradiated by a 248 nm KrF excimer laser (FWHM$\sim$16 ns). $\lambda_{probe}=632.8$ nm, p polarized, $\theta=46°$. Curves represent the spline fit of the experimental data (symbols).

peak corresponds to the transition time t_{tr}, we could estimate the bubble growth velocity. We observe $t_{tr}\sim45$ ns for IPA and ~25 ns for water using a 752-nm probe laser (see Fig. 2). Accordingly, with $R_{tr}\sim87$ nm for IPA ($n_{liq}=1.38$) [10] and $R_{tr}\sim90$ nm for water ($n_{liq}=1.33$) [10], this corresponds to a bubble growth velocity of ~1.9 m/s for IPA and ~3.6 m/s for water. The growth velocities so estimated for other investigated liquids are also found to be in this range, showing a trend in qualitative agreement with the predictions for the inertia-controlled bubble growth [1,6]. It is noted that the Rayleigh formulation for the inertia-controlled bubble growth has been explored at longer, microsecond time scales [1].

Since R_{tr} depends linearly on the probe beam wavelength [7,8], it is expected that the peak position shifts with varying probe beam wavelength. To prove this, we have probed the same spot on the chromium surface with two different lasers (632.8 and 752 nm) under similar conditions, i.e., angle of incidence and polarization. The results for IPA are shown in Fig. 5. With the growth velocity of bubbles for IPA being 1.9 m/s, R_{tr}(632.8 nm)$\sim$73 nm, and R_{tr}(752 nm)$\sim$87 nm, a time shift of $\sim$7 ns is expected between the peak position for the two reflectance signals. The observed value $\sim$8 ns is comparable to this prediction and supports our interpretation that the reflectance transient represents the bubble growth dynamics.

By plotting the amplitude of the reflectance drop versus the excimer laser fluence we can determine the threshold fluence accurately. The results for the test liquids are shown in Fig. 6. The threshold fluences determined from this plot are listed in Table I together with the boiling points for the liquids and the maximum temperatures at the liquid/chromium interface predicted by the calculations for the heat diffusion equation based on the finite-difference method [11,12]. The calculations are performed using the measured reflectivity value, 0.19 at 248 nm, of the Cr film in air, determined by Perkin-Elmer Lambda 6 Spectrophotometer and using the thermal properties of bulk Cr from the literature [10]. The optical properties of evaporated thin Cr film are, in general, different from those of bulk Cr [13,14]. The results indicate that the threshold fluence is sufficient to superheat the liquid tens of degrees above the boiling point. It is noted that uncertainties may be involved in the computation due to the assumed thermal and optical properties for the thin Cr film, which may in reality be different from those of bulk Cr. Above a certain liquid-dependent threshold fluence the reflectance drop appears to saturate. This can be explained by considering that the bubbles grow large enough to touch each other and agglomerate into a continuous vapor film at the liquid/solid interface. The agglomeration is enhanced by increasing number density of embryonic bubbles with increasing laser

TABLE I. The 248-nm KrF excimer laser threshold fluences for the onset of nucleation for different liquids, F_{th}, the boiling points (bp) (Refs. [6,10,15]), and the maximum temperatures at the liquid/chromium interface, T_{max}, calculated for the corresponding threshold fluences (present work).

Liquid	F_{th} (mJ/cm^2)	bp (K)	T_{max} (K)
Ethanol	14.9	351.5	375
Methanol	15.4	337.9	377
IPA	15.7	355.6	379
50:50 water:IPA	19.1	369.8	390
75:25 water:IPA	23.1	371.9	408
85:15 water:IPA	25.9	372.5	420
Water	27.4	373.2	426

fluence. It is known that the number density of the embryonic bubbles increases exponentially with superheat temperature [1,6]. We further observe that the threshold fluence for water-IPA mixtures depends nonlinearly with the alcohol concentration (volume percent). This is consistent with the fact that the properties of liquid mixtures do not depend linearly on the volume or mole fraction of their constituents [15].

We thank D. H. Choi, F. Lee, P. T. Leung, D. Krajnovich, and I. K. Pour of IBM Almaden Research Center, W. Zapka of IBM GMTC, Germany, and J. Boneberg of the University of Konstanz, Germany, for their valuable support, assistance, and contributions to this work. O.Y. would like to acknowledge the financial support from the Friedrich-Ebert-Stiftung, Bonn, Germany. Support to this work by the Computer Mechanics Laboratory of the University of California at Berkeley is gratefully acknowledged.

[1] See, e.g., V. P. Scripov, E. N. Sinitsyn, P. A. Pavlov, G. V. Ermakov, G. N. Muratov, N. V. Bulanov, and V. G. Baidakov, *Thermophysical Properties of Liquids in the Metastable State* (Gordon and Breach, New York, 1988); see also, V. P. Scripov, *Metastable Liquids* (Wiley, New York, 1974).

[2] J. G. Eberhart, J. Colloid Interface Sci. **56**, 262 (1976).

[3] A. C. Tam, N. Do, L. Klees, P. T. Leung, and W. P. Leung, Opt. Lett. **24**, 1809 (1992), and references therein.

[4] A. C. Tam, W. P. Leung, W. Zapka, and W. Ziemlich, J. Appl. Phys. **71**, 3515 (1992).

[5] J. Bodensohn, S. Klesy, and P. Leiderer, Europhys. Lett. **8**, 59 (1989).

[6] V. P. Carey, *Liquid-Vapor Phase-Change Phenomena* (Hemisphere, Washington, 1992).

[7] H. C. van de Hulst, *Light Scattering by Small Particles* (Dover, New York, 1981).

[8] M. Born and E. Wolf, *Principles of Optics* (Pergamon, Oxford, 1991).

[9] J. C. Maxwell Garnett, Philos. Trans. R. Soc. London **203** (1904).

[10] *CRC Handbook of Chemistry and Physics*, edited by R. C. Weast (CRC Press, Boca Raton, 1987), 68th ed.

[11] P. T. Leung, N. Do, L. Klees, W. P. Leung, F. Tong, L. Lam, W. Zapka, and A. C. Tam, J. Appl. Phys. **72**, 2256 (1992).

[12] H. K. Park, X. Xu, C. P. Grigoropoulos, N. Do, L. Klees, P. T. Leung, and A. C. Tam, Appl. Phys. Lett. **61**, 749 (1992).

[13] G. Henderson and C. Weaver, J. Opt. Soc. Am. **56**, 1551 (1966).

[14] *Handbook of Optical Constants of Solids, I*, edited by E. D. Palik (Academic, New York, 1985).

[15] L. E. Nielsen, *Predicting the Properties of Mixtures* (Marcel Dekker, New York, 1978).